Anomalous solubility behavior of mixed monolayer protected metal nanoparticles

by

Jacob W. Myerson

Submitted to the Department of Materials Science and Engineering in Partial Fulfillment of the Requirements for the Degree of

Bachelor of Science

at the

Massachusetts Institute of Technology

June 2005

Signature of Author.....
Department of Materials Science and Engineering
May 13, 2005

Certified by.....
Francesco Stellacci
Finmeccanica Assistant Professor of Materials Science and Engineering
Thesis Supervisor

Accepted by.....
Donald Robert Sadoway
John F. Elliott Professor of Materials Chemistry
Chair, Undergraduate Thesis Committee

ANOMALOUS SOLUBILITY BEHAVIOR OF MIXED MONOLAYER PROTECTED METAL NANOPARTICLES

by

JACOB W. MYERSON

Submitted to the Department of Materials Science and Engineering
on May 13, 2005 in Partial Fulfillment of the
Requirements for the Degree of Bachelor of Science in
Materials Science and Engineering

ABSTRACT

The solubility of mixed monolayer protected gold nanoparticles was studied. Monolayer protected metal nanoparticles are attractive materials because of the optical and electronic properties of their metal cores and because of the surface properties of their ligand coating. Recently, it was discovered that a mixture of ligands phase separate into ordered domains of single nanometer or subnanometer width on the surface of metal nanoparticles. The morphology and length of the ligand domains (which take the form of ripples on the particle surface) has given these nanoparticles novel properties.

Because monolayer protected nanoparticles can be dissolved and dried many times, they can be handled and processed in ways not available to other nanomaterials. Understanding the solubility of mixed monolayer protected metal nanoparticles could help in implementing their unique new properties. This study demonstrates that the solubility of these particles in organic solvents cannot be explained only in terms of the composition of the ligand shell. Instead, solubility is also closely linked to morphology of the ligand shell via relationships between the size of the solvent molecule and the size of the features in the morphology.

Thesis Supervisor: Francesco Stellacci
Title: Finmeccanica Assistant Professor of Materials Science and Engineering

Table of Contents

List of Figures

ACKNOWLEDGEMENTS

I express my deepest gratitude to Prof. Francesco Stellacci for his uncommonly faithful support through two years of research. He is responsible for most all of my knowledge of and interest in nanoscience and has shown great patience in taking extensive lengths to assure that I can come away from MIT as a better researcher. I also thank all members of professor Stellacci's research group, past and present. Each has at some point encouraged me socially, academically, or professionally, and all have been available for scores of questions. Additionally, Benjamin Wunsch deserves thanks for his help with TEM images. Special thanks are due to Alicia Jackson for her help with STM images and for her research that led to the first characterization of "rippled" nanoparticles.

Chapter 1. Introductory Remarks

Metal-core nanoparticles are an attractive class of nanoscale materials because of their optical, electronic, and sensing properties [1]. Metal nanoparticles have shown single electron transistor behavior and surface plasmon resonance tuning and sensing [2,3]. The Brust-Schiffrin method has provided a simple way to synthesize gold or silver nanoparticles coated with a monolayer of thiolated ligands [4,5]. With monolayer-protected metal nanoparticles (MPMNs), the ligand shell that coats the particle surface stops the gold nanoparticles from coalescing, both in solution and in solid state [6]. Furthermore, the organic molecules provide most of the particles' surface related properties, including sensing and assembly properties [1,6,7]. The ligands also provide the particles with solubility. In fact, MPMNs approximate the behavior of organic molecules. They can be dried and re-dissolved many times and can be purified via dialysis, chromatography or filtration [7].

Solubility is an important property of these nanoparticles. Soluble nanoparticles can be processed and handled in ways that are not possible for other nanomaterials. Previous studies have investigated the solubility of nanoparticles in polar solvents like water [8]. For particles in polar solvents, the main mechanism that provides stability is the formation of an electrical double layer. The electrical double layer is less important to the solubility of nanoparticles in non-polar solvents [8]. Though MPMN solubility in apolar solvents is not well understood, it is commonly believed that it depends only on the type of molecules in the ligand shell. However, for the case of monolayer protected silver nanoparticles, studies have shown that factors other than ligand shell composition, including the Gibbs free energy of interdigitation, must be considered in determining solubility [9].

A recent study demonstrates that a mixture of thiolated molecules that might normally phase separate into randomly shaped domains on a flat surface can assemble into ordered domains on the surface of a nanoparticle. For a mixture of two types of thiol, stripes of alternating ligand type appear. The stripes, or "ripples," are as small as 5 Å in width and extend around the circumference of the nanoparticles. Nanoparticles coated with a binary mixture of thiols are thus a new type of material that is both nanosized and nanostructured. This unique combination of morphologies has already hinted at some novel materials properties, including resistance to nonspecific adsorption of proteins [10].

Previous work has shown that the ligand shell morphology also impacts the solubility of these particles [10]. Indeed, the solubility of "rippled" nanoparticles is not simply function of ligand shell composition and does not appear to be explicable via a simple Gibbs free energy of miscibility consideration. Instead, this study shows that there is a close and complex relationship between solubility and morphology of the ligand shell. The study will attempt to characterize the solubility of rippled nanoparticles as a function of both ligand shell composition and ligand shell morphology. A basic knowledge of this relationship could be fundamental to using mixed ligand coated metal nanoparticles for their novel properties.

Chapter 2. Background Information

Metal, metal-oxide, or semiconductor colloids and nanocrystals are important types of nanoscale materials. They consist of particles with typical diameters in the range of 1-20 nm. Due to their small dimensions, nanoparticles have unique properties, including superparamagnetism, fluorescence with high quantum yields, and low melting points. Nanoparticles can thus easily be employed in biological labeling and sensing as well as many other applications involving optical, electronic, or magnetic components on a small scale [6].

A large fraction of the atoms in metal nanoparticles are at the particle surface. Thus, when a monolayer of thiols is deposited on a nanoparticle surface, there is an intimate connection between the properties of the monolayer and the properties of the nanoparticle [6]. Self-assembled monolayers (SAMs) are single-molecule layers on surfaces. The molecules in SAMs consist of an end that can chemically bond to a surface, a molecular backbone, and a molecular head group that determines the surface properties of the monolayer. The molecules in an SAM can also provide new properties to the surface that they coat. Monolayer protected metal nanoparticles (MPMNs) consist of a nanosized metallic core with an SAM its surface. These particles have properties stemming from the SAM, from the metallic core, and from combinations of the two. The monolayer coating provides the particles with most surface properties, including a heavy contribution to determining the solubility of the particles [2, 3, 7, 10].

The Brust-Schiffrin method is a common and simple way to synthesize metallic gold nanoparticles functionalized with thiols [4,5]. The synthesis reaction can take place in a one-phase (ethanol) or two-phase (water and organic) system [7,11]. A gold salt ($HAuCl_4$) is dissolved in the same phase as the ligands that will make the nanoparticle shell. Via the

reaction shown in equation (1), the gold reacts with thiolated ligands to form an intermediate Au(I)-thiol polymer. A reducing agent ($NaBH_4$) is added, reducing the gold ions according to equation (2). The gold ions form small clusters that combine with the ligands as they grow. Once the entire surface of a cluster is coated in ligands, the cluster stops growing. The initial molar ratio of ligands to gold determines the size of the nanoparticles. Thus, the Brust-Schriffin method allows for simple control over the core size and ligand nature of MPMNs. A one to one molar ratio of ligands to gold defines the size of all nanoparticles studied in this work [6].

$AuCl_4^-$(toluene) + RSH → (--Au^ISR--)$_n$(polymer) *equation (1)*

(--Au^ISR--)$_n$ + BH_4 → Au_xSR_y *equation (2)*

A mixed-ligand SAM can be made either by absorption of ligands from a solution of two or more types of molecule or by placing an existing monolayer into a solution containing appropriate molecules not found in the original monolayer [12,18]. Scanning tunneling microscopy (STM) images have shown that some mixed SAMs have phase-separated regions containing only one type of molecule. However, these regions are not arranged via any discernible ordering [12-16].

A variation on the Schiffrin method allows for synthesis of gold nanoparticles coated with a mixed SAM [9,17]. The MPMNs used in this study employ a mixture of two types of ligand, one with a hydrophobic head group and one with a hydrophilic head group, and are created via the former of the two abovementioned methods.

For these binary mixtures of ligands, "ripples" of alternating ligand composition appear in the ligand shell of the gold nanoparticles. "Ripples" are phase-separated ligand domains that forms rings around the nanoparticles. The spacing between ligand rings of the same composition varies one molecular layer at a time as a function of the stoichiometric ratio of

ligand types. The molar ratio between ligand types can also, for especially high or low ratios, change or eliminate the ordering of domains. The 'depth' of the ripples is determined by the difference in the lengths of the two ligands that form the domains [Figure 1]. The formation of the ordered domains is also known to depend on the curvature of the surface on which the thiol mixture assembles. The features in the ligand shell of rippled nanoparticles, which can be of subnanometer scale, provide the nanoparticles with unique new properties, including novel solubility results [10].

A simple analysis of the solubility of MPMNs might consider the solubility of the head groups in the ligand shell as the determining factor in the solubility of the nanoparticle. A Gibbs free energy of miscibility analysis along these lines can predict that nanoparticle solubility depends linearly on the amount of one type of head group (and thus ligand) in the ligand shell. For example, under this analysis, a nanoparticle coated in a binary mixture of alkyl-terminated ligands and carboxylic acid-terminated ligands would be more soluble in a hydrophilic solvent with more carboxylic acid head groups in its ligand shell.

However, the spacing between domains on the surface of a rippled nanoparticle is consistently small enough that it becomes comparable to the size of a solvent molecule. Solvent molecules may interact directly with the morphology in the ligand shell of rippled nanoparticles. Indeed, preliminary study of the solubility of rippled nanoparticles in ethanol has shown a non-linear relationship with ligand shell composition [10].

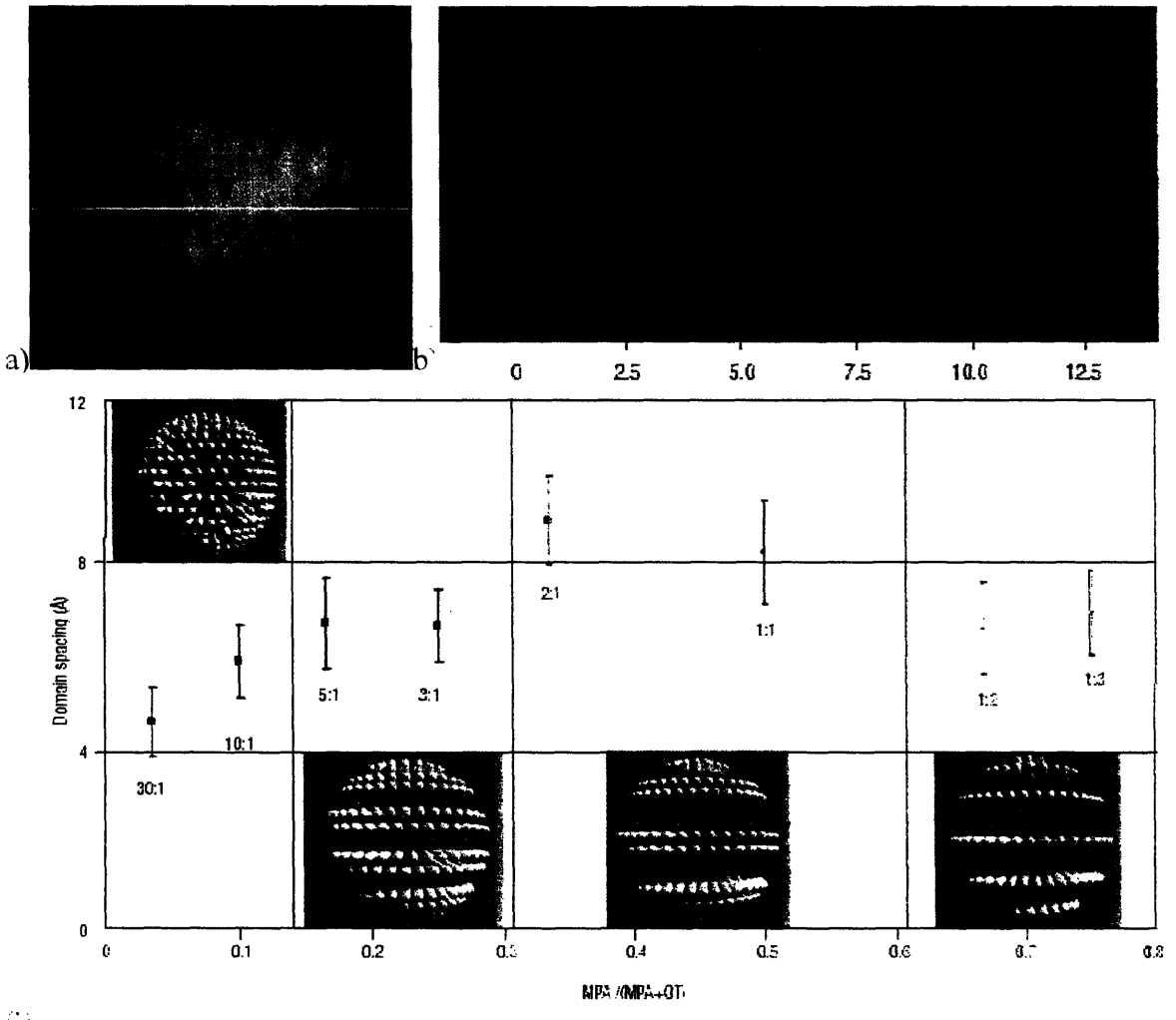

Figure 1. a) STM image showing ripples on the surface of a gold nanoparticle coated by a mixture of octanethiol and mercaptopropionic acid in stoichiometric ratio 2:1 [10]. b) Cross-section of (a) with a nanometer scale bar showing the ripple spacing to be on the order of 1 nm [10]. c) Schematic showing how domain spacing can vary in rippled nanoparticles via alteration of the stoichiometric ratio of ligands types coating the nanoparticle [10]

Chapter 3. Experimental Methods

3.1 Materials

The chemicals used in the synthesis of gold nanoparticles were hydrogen tetrachloroaurate trihydrate, sodium borohydride, and thiolated ligands (octanethiol (CH_3-(CH_2)$_7$-SH, OT), hexanethiol (CH_3-(CH_2)$_5$-SH, HT), mercaptopropionic acid (HOOC-(CH_3)$_2$-SH, MPA), and mercaptoundecanoic acid (HOOC-(CH_3)$_{10}$-SH, MUA)). Octanedithiol was used in the preparation of monolayers of nanoparticles for scanning tunneling microscopy. Gold foil was used as a substrate for assembly of such monolayers. Hydrochloric acid was used to protonate charged ligands on nanoparticles. Each chemical was purchased from Sigma-Aldrich and used as received. The solvents used in synthesis, sample preparations, and solution preparations were acetone, ethanol, toluene, 1-propanol, isopropanol, methanol, acetonitrile, dichloromethane, and hexanes. Each was purchased from VWR.

3.2 Synthesis of Gold Nanoparticles

Gold nanoparticles were synthesized according to a modified version of Schiffrin's method in which the particles are synthesized in one phase, rather than two. 0.9 mmol of hydrogen tetrachloroaurate (354 mg) were dissolved in 200 ml of ethanol kept at 0 ^{0}C. A mixture of thiols in a fixed molar ratio was added so that the total ligand concentration was kept at 0.9 mmol. 200 ml of a sodium borohydride (.132 mol/L) ethanol solution were slowly added dropwise. The solution was left stirring for two hours and then stored in a refrigerator overnight, during which time a black precipitate formed. The precipitate was separated by filtration over quantitative paper filter and washed many times with acetone, ethanol and water

to remove unreacted ligands or excess sodium borohydride. Typically, ~100 mg of a black powder were obtained. The powder was stored in a refrigerator. For all nanoparticles, the ligands consisted of a mixture of an alkyl-terminated thiol and an acid-terminated thiol. Particles were synthesized with ligand mixtures consisting of OT and MPA, OT and MUA, and HT and MUA. For each type of mixture, particles were synthesized with ten different moles acid : moles alkyl ratios (1:20, 1:10, 1:5, 1:2, 1:1, 2:1, 3:1, 5:1, 10:1, and 1:0 (moles acid/moles alkyl)).

3.3 Preparation of Nanoparticle Solutions

As obtained after synthesis, the nanoparticles were not soluble in organic solvents due to deprotonation of acid groups by sodium borohydride to form highly polar carboxylate end groups in the ligand shell. 1 mg of nanoparticles was suspended in ethanol (~2ml) via sonication. One drop of hydrochloric acid was added to form sodium chloride and reduce the sodium carboxylate end groups into carboxylic acid. The nanoparticle solution was quickly dried, forming a crystal on the inner surface of the solution vessel. The dried solid was washed extensively with deionized water to remove salt precipitates. After removal of water, the desired solvent (Toluene, ethanol, 1-propanol, isopropanol, or methanol) was added in an amount that assured a nanoparticle concentration of 1 mg/10 ml solvent. The new solution was sonicated for fifteen minutes and stirred for three hours. After stirring, the solution was given one week to settle before further use.

3.4 Characterization of Gold Nanoparticles

Morphologies in the nanoparticles' ligand shells were characterized with STM. A solution of 1 mg of nanoparticles in 10 ml of an appropriate solvent (usually ethanol or toluene) was prepared according to a version of the above method without stirring or decanting time. .1 mg of octanedithiol was added to the solution, which was subsequently sonicated for an additional two minutes. 1 cm^2 of gold foil was sonicated in acetone for twenty minutes, dried, and placed in the nanoparticle and octanedithiol solution overnight. The gold foil was then given two hours to rinse in ethanol, toluene, dichloromethane, methanol, and acetonitrile. The monolayer of nanoparticles on the gold was imaged via scanning tunneling microscopy (STM) with a Digital Instruments Multimode NanoScope 3A scanning probe microscope. Multiple locations on each sample were imaged with different scan angles, z-limits, and magnifications. Images were captured with Digital Instruments NanoScope III software, version 5.12b48.

The core size of the nanoparticles was examined with transmission electron microscopy (TEM) images obtained using a JEOL 2010 microscope operating at 200 kV. In order to prepare samples for TEM imaging, the solvent was evaporated from small amounts of nanoparticle solutions deposited on 200-mesh carbon-coated copper TEM grids (LADD Research). TEM images were scanned and nanoparticle diameters were measured using NIH's ImageJ software.

3.5 Characterization of Nanoparticle Solubility

The solubility of the nanoparticles was evaluated through an optical absorption spectrum obtained using a Cary 5E spectrophotometer (Varian) over a wavelength range of 400-700 nm. The focus of the analysis was the absorption peak at ~520 nm, corresponding to

surface plasmon resonance of the nanoparticles in solution. The optical absorption intensity at the plasmon resonance wavelength is known to be directly proportional to the number of nanoparticles in solution. This value was thus taken as a measure of the solubility of the nanoparticles.

Chapter 4. Results and Discussion

The study is aimed at showing the relationship between the solubility of MPMNs coated with a binary mixture of ligands and the composition and morphology of the ligand shell of said MPMNs. Therefore, a number of ligand shell variables were considered in synthesizing the tested nanoparticles. To begin with, the ratio between the number of alkyl-terminated ligands and the number of acid-terminated ligands was varied between ten values. In this way, the width of the features in the ordered ligand-shell morphology was varied and ordering itself was reduced or eliminated at the highest or lowest ligand ratios. Additionally, variation in ligand composition, regardless of morphology, changes the properties of the nanoparticle surface. In this case, said variation introduces more or less hydrophilic head groups to the ligand shell.

While the molar ratio between acids and thiols is responsible for many variables in this study, different combinations of ligands were also considered for their impact on the ligand shell and, by extension, solubility. For one, two classes of rippled nanoparticles were synthesized, those in which MUA, an acid, represents the longest ligand and those in which OT, a thiol, represents the longest ligand. Additionally, amongst particles with MUA as the acid, ten particles were synthesized with OT as the thiol and ten counterpart particles were synthesized with HT as the thiol. MPMNs coated in HT and MUA have 'deeper' ripples than those coated with OT and MUA because HT is a shorter molecule than OT.

Finally, since the size of the features on the MPMNs may match the size scale of solvent molecules, size and shape of solvent molecules were considered in the choice of tested solvents. Nanoparticle solubility in four alcohols (isopropanol, 1-propanol, ethanol, and methanol) was tested. The alcohols were chosen to represent three different lengths of

molecule and, in the case of isopropanol, a larger and 'rounder' molecule. Toluene solubility was also tested in order to study nanoparticle solubility in a mostly apolar solvent and compare results to solubility in the more polar alcohol solvents.

4.1 Nanoparticle Sizes Evaluated via TEM Imaging

TEM was used to evaluate the core size of the nanoparticles. Images were obtained for seven types of particle and average nanoparticle diameter was calculated for each. The goal in the evaluation of core sizes is to assure that similar core sizes were present for each type of nanoparticle. Indeed, the average nanoparticle sizes for each type of particle examined were 7.81nm, 8.02nm, 7.56nm, 9.56nm, 10.05nm, 10.09nm, and 10.20nm [Figure 2]. Given these similar core sizes across the range of tested samples, size effects can reasonably be eliminated from discussion comparing solubility results in different samples. Additionally, it may be assumed that the absorption optical cross-section is the same across the series of nanoparticles.

4.2 Ligand Shell Morphology Evaluated via STM Imaging

STM images were used to make some basic characterizations of ligand shell morphology in the tested nanoparticles. The goal in the imaging was to verify that ordered ligand domains could form on the surface of nanoparticles for multiple ligand shell compositions given a binary ligand mixture of OT and MUA or of HT and MUA. Previous work has extensively characterized the formation of ripples in ligand shells composed of OT and MPA. Previous study has also noted the formation of ripples for some particles coated in MUA and OT or MUA and HT [10]. Images produced for this study have verified the

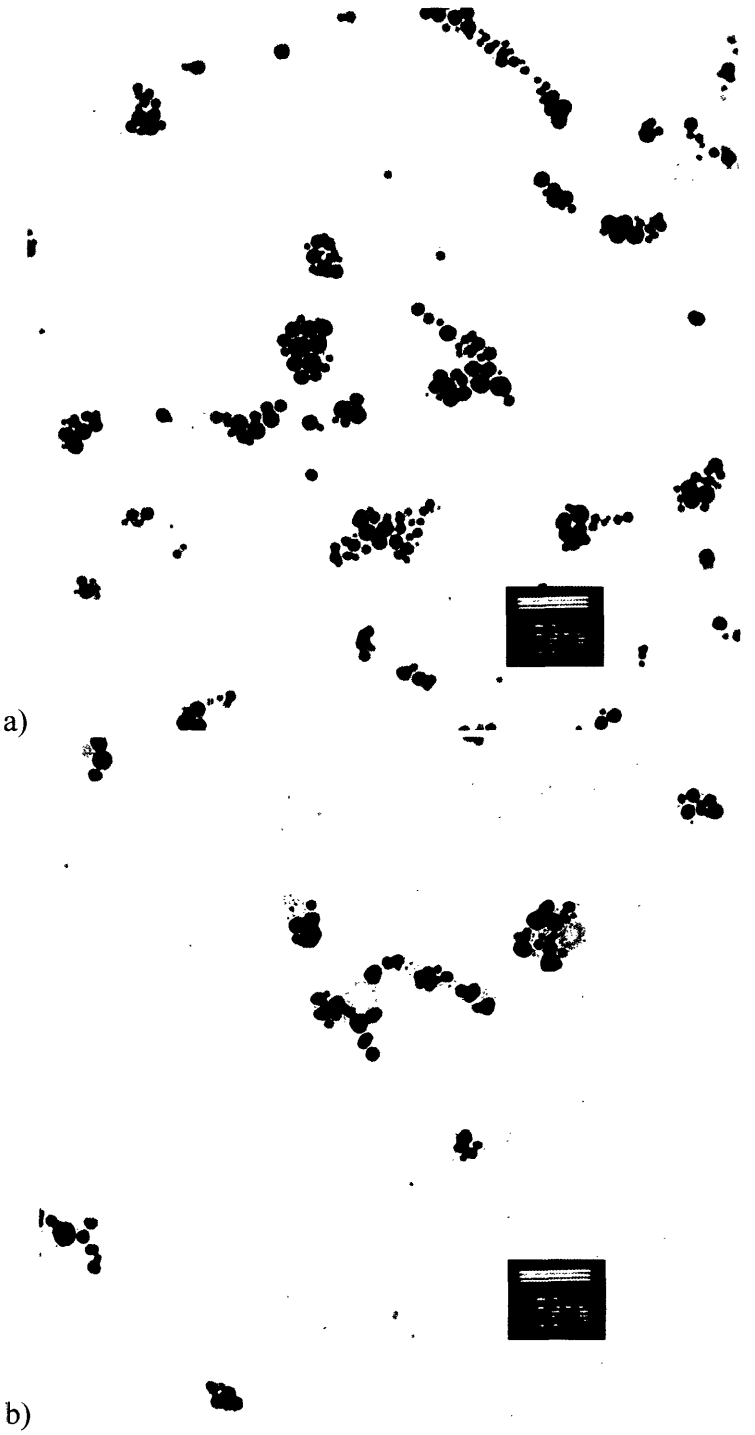

a)

b)

Figure 2. a) TEM image of nanoparticles with ligand coating 1 mol HT/ 2 mol MUA and average nanoparticle diameter of 10.20 nm, b) TEM image of nanoparticles with ligand coating 2 mol HT/ 1 mol MUA and average nanoparticle diameter of 10.09 nm

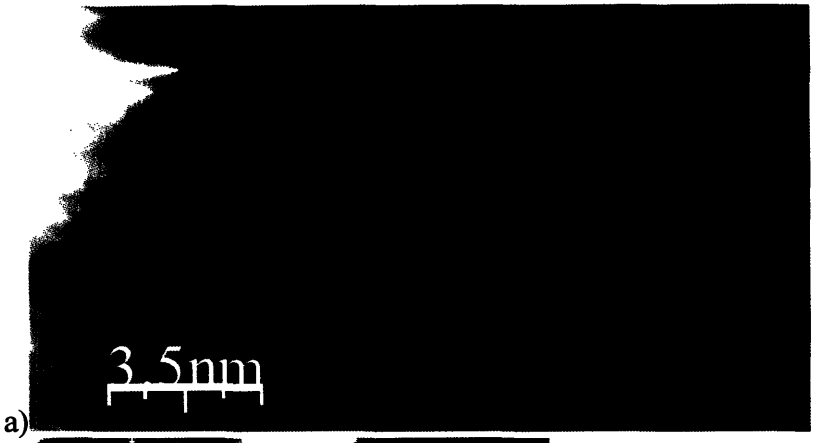

a)

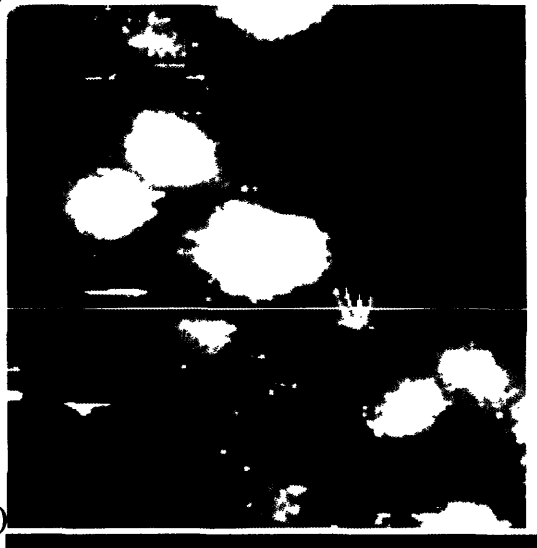

b)

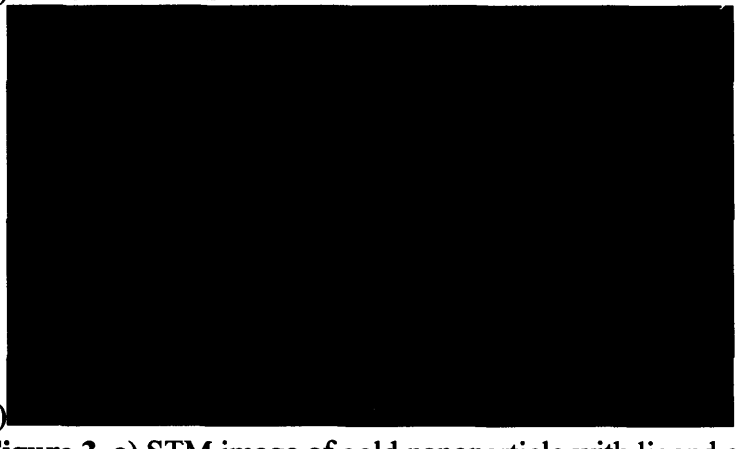

c)

Figure 3. a) STM image of gold nanoparticle with ligand coating 1 mol OT/1 mol MUA, b) STM image of gold nanoparticles with ligand coating 1 mol HT/1 mol MUA, c) Cross section of (b) showing possible ripples with the red markers

previous characterizations and offer evidence that ripples will form in ligand shells composed of OT and MUA or of HT and MUA assembled on a gold nanoparticle surface [Figure 3]. Ripples were not likely to form when the percentage of one molecule in the ligand shell far exceeded the percentage of the other.

4.3 Solubility of Nanoparticles Coated with OT and MPA

For particles coated with a mixture of OT and MPA, the carboxylic acid terminated molecules were the shorter of the two. When ripples form from OT and MPA, the hydrophilic component to the ligand shell is thus deeper set in the ligand morphology. For hydrophilic solvents to dissolve these particles, it would be expected that the solvent molecules would need to interact with the ripple morphology by reaching into the deeper ligand domains.

Within the scope of this study, the relationship between solubility and ligand shell morphology in particles coated in OT and MPA is still poorly understood. Solubility results present a behavior that does not appear to correspond to a relationship with composition or morphology in any direct way. In fact, the nanoparticles were insoluble or nearly insoluble in organic solvents for almost all tested ligand shell compositions [Figure 4].

Fourier transform infrared spectroscopy data indicate that hydrochloric acid does not always successfully protonate the carboxylates on MPA in ligand shells where ordered domains are apparent. That is, the charged carboxylates on MPA-coated nanoparticles are not always neutralized during the process described in the methods. The presence of carboxylates in the ligand shell of OT and MPA coated nanoparticles is likely responsible for their insolubility in organic solvents. The charge due to carboxylates skews solubility data and

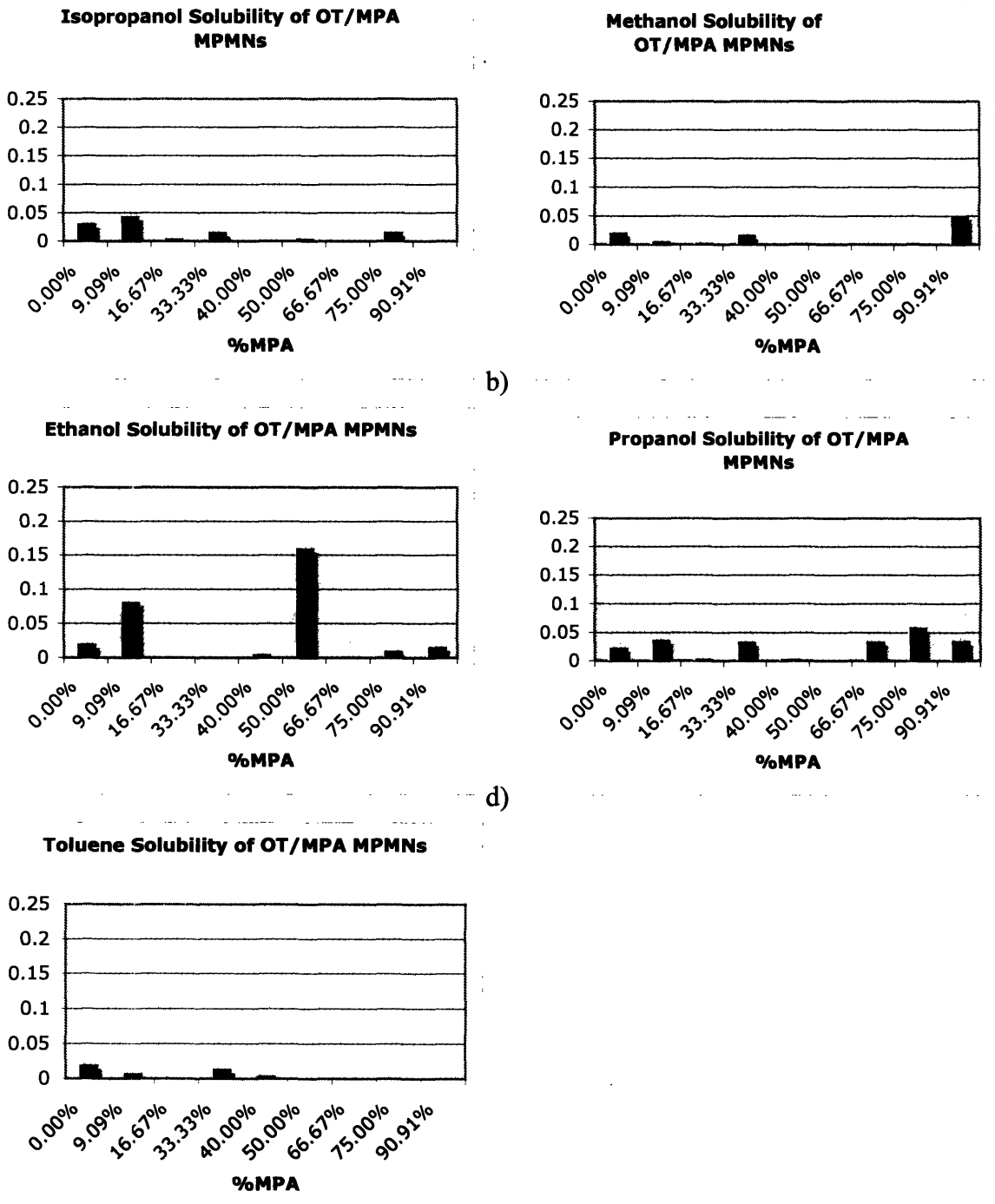

Figure 4. a) Plot of solubility (determined via optical absorbance intensity at plasmon resonance as described in the methods) of OT/MPA nanoparticles in isopropanol, b) Plot of solubility of OT/MPA nanoparticles in methanol, c) Plot of solubility of OT/MPA nanoparticles in ethanol, d) Plot of solubility of OT/MPA nanoparticles in propanol, e) Plot of solubility of OT/MPA nanoparticles in toluene

makes it difficult to draw conclusions as to the relationship between the solubility of the nanoparticles and their ligand shell composition and morphology.

4.4 Solubility of Nanoparticles Coated with HT and MUA

As indicated in the background section, a Gibbs free energy of miscibility analysis of mixed monolayer protected metal nanoparticles leads to the prediction that the solubility of the nanoparticles depends linearly on ligand shell composition. In the case of particles coated with HT and MUA, the addition of more MUA to the ligand shell would theoretically result in a linear increase in the solubility of the particles in a polar solvent such as ethanol. Additionally, at or below a minimum concentration of MUA in the ligand shell, the nanoparticles would theoretically be insoluble in ethanol. The inverse behavior would be expected for solubility in an apolar solvent like toluene.

This expected solubility behavior is not evident. Indeed, ethanol solubility does not increase monotonically with the addition of MUA to the ligand shell. Instead, ethanol solubility reaches a peak value for a ligand shell composed of 33.33% MUA. For larger percentages of MUA, ethanol solubility actually decreases. Rather than a monotonically decreasing solubility profile with respect to MUA content, 'oscillatory' behavior is observed in the case of toluene solubility. Particles with 66.66% and 33.33% MUA in their ligand shell are highly toluene soluble while particles with 50% MUA are mostly toluene insoluble. Although particles with 66.66%, 90.91%, and 100% MUA are insoluble in toluene, particles with 83.33% MUA are somewhat toluene soluble. Neither toluene nor ethanol solubility behavior was predicted and neither was explainable within the boundaries of present solubility theories [Figure 5].

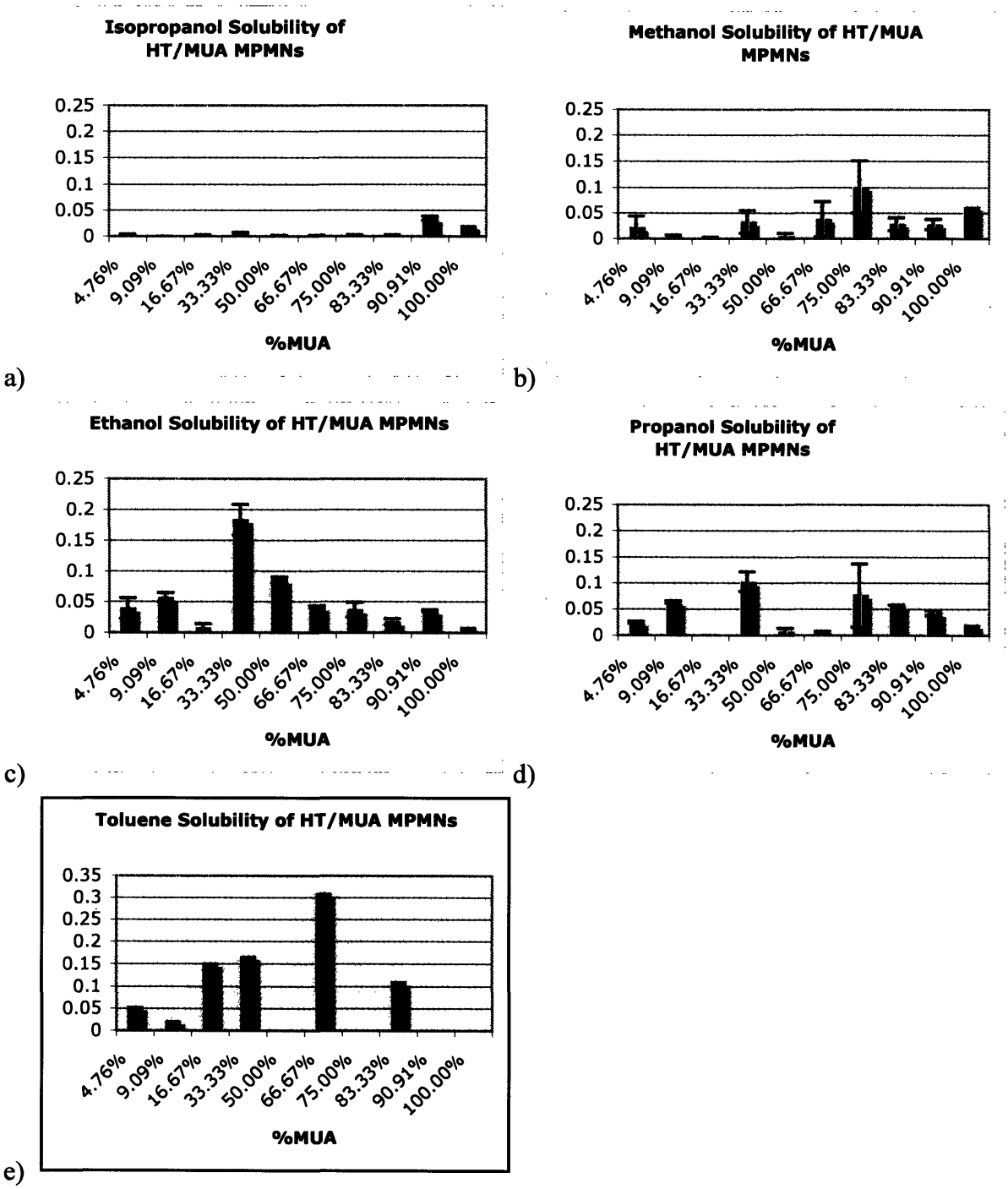

Figure 5. a) Plot of solubility (determined via optical absorbance intensity at plasmon resonance as described in the methods) of HT/MUA nanoparticles in isopropanol, b) Plot of solubility of HT/MUA nanoparticles in methanol, c) Plot of solubility of HT/MUA nanoparticles in ethanol, d) Plot of solubility of HT/MUA nanoparticles in propanol, e) Plot of solubility of HT/MUA nanoparticles in toluene

In order to better investigate this anomalous behavior in the context of ripple size, the solubility of HT/MUA particles in a series of alcohols was studied. The particles are almost insoluble in isopropanol, a molecule that is too bulky to penetrate into the ripples. The solubility in methanol, a small and highly polar molecule, is almost constant and near zero for ligand shells containing 50% or less MUA. Methanol solubility somehow increases as more MUA is present in the ligand shell, showing generally higher values for greater than 50% MUA in the ligand shell and generally lower values for less than 50% MUA. Non-monotonic or oscillatory behavior is observed when dissolving the particles in solvents like ethanol or propanol, which are composed of elongated molecules with a hydrophobic tail and a hydrophilic head. These molecules are able to penetrate the ripples and their interactions with them must depend on ripple spacing in relation to the molecular dimensions. As mentioned, ethanol solubility reaches a peak value for 33.33% MUA coated nanoparticles. Propanol solubility also reaches a high point for 33.33% MUA ligand composition and follows a pattern with respect to composition that is roughly similar to the pattern in ethanol solubility. In general, though, the nanoparticles at any given ligand shell compositions are less soluble in propanol than in ethanol.

4.5 Solubility of Nanoparticles Coated with OT and MUA

An additional variable that was controlled for this study was the ripple 'depth,' defined as the height difference between the long and the short ligands. HT is shorter than OT, particles covered in OT and MUA were examined alongside HT/MUA particles as an example of 'shallower' ripples.

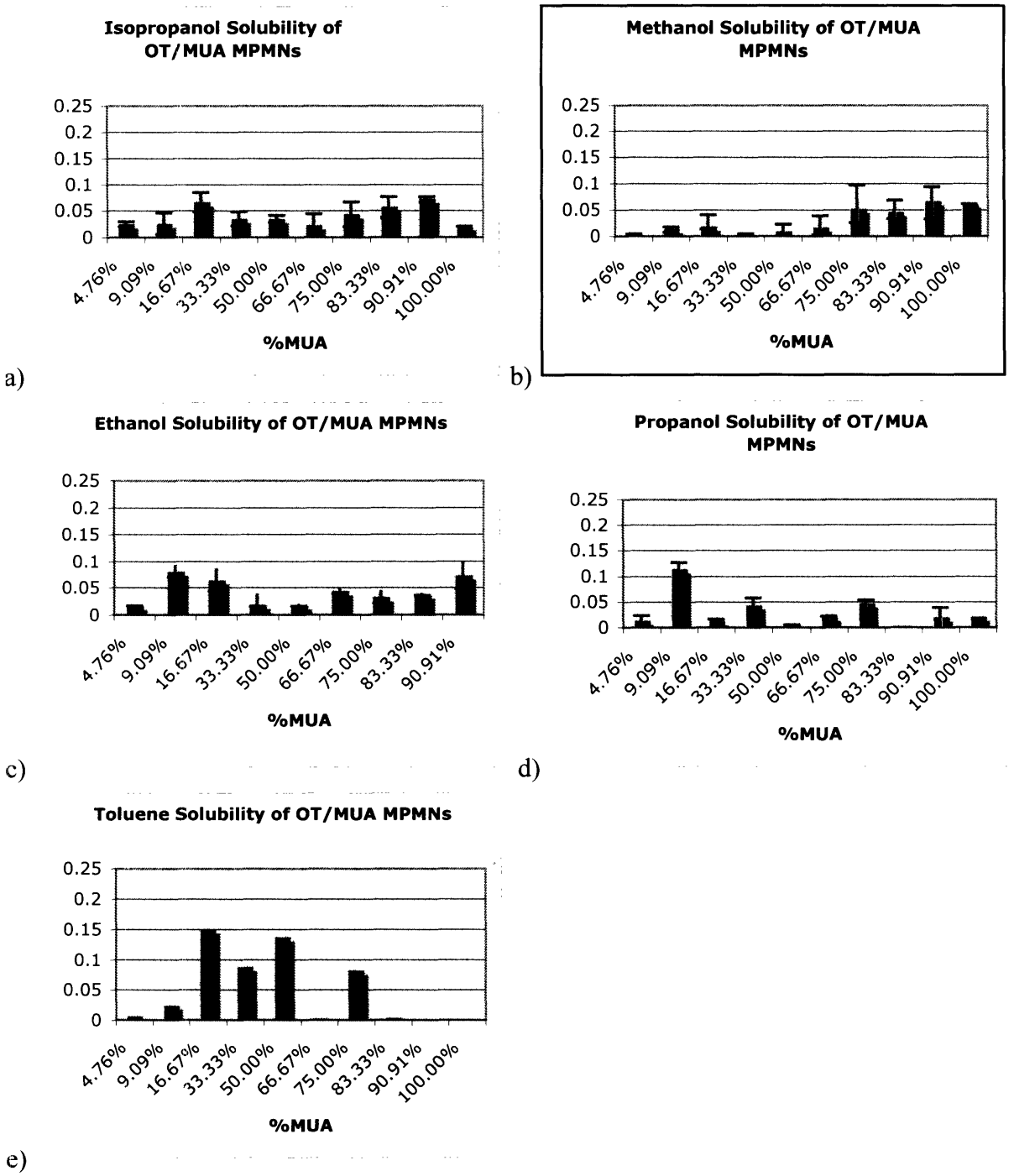

Figure 6. a) Plot of solubility (determined via optical absorbance intensity at plasmon resonance as described in the methods) of OT/MUA nanoparticles in isopropanol, b) Plot of solubility of OT/MUA nanoparticles in methanol, c) Plot of solubility of OT/MUA nanoparticles in ethanol, d) Plot of solubility of OT/MUA nanoparticles in propanol, e) Plot of solubility of OT/MUA nanoparticles in toluene

For OT and MUA-coated nanoparticles, solubility in isopropanol and in methanol shows behavior similar to that seen with particles coated in HT and MUA. Isopropanol solubility is slightly enhanced by the change to OT in the ligand shell, but methanol solubility maintains the pattern of increasing from nearly zero solubility to moderate solubility as more MUA is added to the coating [Figure 6].

The behavior of ethanol solubility changes drastically in switching between OT and HT in the ligand shell. The solubility of OT/MUA nanoparticles in ethanol in fact resembles the solubility of OT/MUA nanoparticles in isopropanol. Indeed, the 'oscillations' in ethanol solubility seen for HT and MUA ligand shells have been weakened by the transition to shallower ripples. With HT as the alkyl-terminated ligand, particles coated with 33.33% and 50% MUA are the most soluble in ethanol. With OT replacing HT, analogous particles are almost insoluble in ethanol. For the case of propanol solubility, the transition from HT to OT appears to have only a minor impact on the pattern in solubility with respect to composition. Nonetheless, the propanol solubility of nanoparticles coated with 33.33% MUA does drop from the high value exhibited for HT/MUA particles. Additionally, as compared to nanoparticles with deeper ripples, more ligand compositions result in near insolubility in propanol.

In the case of toluene solubility, the change in ripple depth does not appear to affect the pattern of solubility behavior for ligand shells with less than 50% MUA. Nanoparticles coated in 90.91% MUA are completely insoluble in toluene, regardless of the length of the alkyl-terminated ligand. However, when OT is the alkyl-terminated ligand, toluene dissolves particles with 50% and 75% MUA ligand shells, but fails to dissolve particles with 66.67% and 83.33% MUA ligand shells. In contrast, when HT is the alkyl-terminated ligand, toluene

dissolves particles with 66.67% and 83.33% MUA ligand shells, but fails to dissolve particles with 50% and 75% MUA ligand shells.

Chapter 5. Conclusions and Future Work

In general, monolayer protected metal nanoparticles have a wide range of potential applications and attractive properties that are derived from both their metallic core and from the ligands on their surface. MPMNs have proven to be useful in biological sensing, in self-assembly, and in nanoscale electronic devices. The innovation of a mixed monolayer protected metal nanoparticle with ordered ligand domains on its surface represents the development of a new class of nanoparticle that is both nanosized and nanostructured. The combined properties of an MPMN and subnanometer scale 'ripples' of ligand domains on the MPMN surface have offered promising results for new properties and applications, including resistance to the nonspecific adsorption of proteins [10]. For MPMNs in general, solubility is a useful property that offers options for handling and processing that are unique amongst nanomaterials. Characterizing the solubility of rippled nanoparticles could be fundamental to applying their novel properties and may help to understand how the ripple morphology contributes to functionalizing the surface of the nanoparticles.

This study contradicts a common perception in determining that the composition of the ligand shell of a mixed monolayer protected metal nanoparticle does not alone determine the solubility of said nanoparticle. Indeed, the addition of more of a hydrophilic head group in the ligand shell of rippled nanoparticles does not translate to greater solubility in a polar solvent like ethanol or to lesser solubility in an apolar solvent like toluene. Instead, solubility in some solvents oscillates with varying ligand composition. The ordered morphology of the ligand shell appears to be intimately connected to these solubility results. Isopropanol is too large a solvent molecule to penetrate into the ripples and fails to dissolve most tested nanoparticles.

Solvents like ethanol and propanol have a hydrophobic tail and a hydrophilic head and can penetrate into the ripples. The solubility of nanoparticles in these solvents oscillates with ligand shell composition. Additionally, when one ligand is changed to make the ripples more 'shallow,' oscillations in ethanol and propanol solubility are dampened or dissipated. Solubility in a smaller solvent molecule (methanol) and a larger solvent molecule (isopropanol) is left virtually unchanged by this alteration in morphology.

Further study should include a more thorough investigation of the solubility of rippled nanoparticles for which the longest ligand is acid-terminated. A theoretical framework to explain the solubility of rippled nanoparticles could be innovated as well. Since a Gibbs free energy of miscibility analysis does not sufficiently explain the oscillatory behavior of some solubility results, new terms could be added to this formalism to consider some of the factors brought up in this study, including the interaction between solvent and ligand shell morphology.

References

[1] Daniel, M. C. & Astruc,D. Gold nanoparticles: Assembly, supramolecular chemistry, quantum-size related properties, and applications toward biology, catalysis, and nanotechnology. *Chem. Rev.* **104,** 293–346 (2004).

[2] Link, S. & El-Sayed, M. A. Spectral properties and relaxation dynamics of surface plasmon electronic oscillations in gold and silver nanodots and nanorods. *J. Phys. Chem. B* **103,** 8410–8426 (1999).

[3] Andres, R. P. *et al.* ''Coulomb staircase'' at room temperature in a self-assembled molecular nanostructure. *Science* **272,** 1323–1325 (1996).

[4] Brust, M.; Fink, J.; Bethell, D.; Schiffrin, D.; Kiely, C. J. Synthesis and reactions of functionalized gold nanoparticles *J. Chem. Soc., Chem. Commun.* **16,** 1655 (1995).

[5] Brust, M.; Walker, M.; Bethell, D.; Schiffrin, D.; Whyman, R. Synthesis of thiol-derivatized gold nanoparticles in a 2-phase Liquid-Liquid system. *J. Chem. Soc., Chem. Commun.* **7,** 801 (1994).

[6] Love JC, Estroff LA, Kriebel JK, *et al.* Self-assembled monolayers of thiolates on metals as a form of nanotechnology *Chemical Reviews* **105** (4), 1103-1169 (2005).

[7] Templeton, A. C.,Wuelfing, M. P. & Murray, R. W.Monolayer protected cluster molecules. *Acc. Chem. Res.* **33,** 27–36 (2000).

[8] Oldfield, G; Mulvaney, P. Au@SnO2 core-shell nanocapacitors, *Adv. Mater.*, **12,** 1519-1522 (2000).

[9] Stellacci, F. *et al.* Laser and electron-beam induced growth of nanoparticles for 2D and 3D metal patterning. *Adv. Mater.* **14,** 194–198 (2002).

[10] Jackson, A.M., Myerson, J.W., Stellacci, F. Spontaneous assembly of subnanometre-ordered domains in the ligand shell of monolayer-protected nanoparticles. *Nature Materials* **3**, 330-336 (2004).

[11] Stellacci, F. *et al.* Ultrabright supramolecular beacons based on self-assembly of two-photon chromophores on metal nanoparticles. *J.Am. Chem. Soc.* **125,** 328–328 (2003).

[12] Stranick, S. J. *et al.*Nanometer-scale phase separation in mixed composition self-assembled monolayers. *Nanotechnology* **7,** 438–442 (1996).

[13] Delamarche, E.,Michel, B., Biebuyck, H. A. & Gerber, C. Golden interfaces: The surface of self-assembled monolayers. *Adv. Mater.* **8,** 719–724 (1996).

[14] Folkers, J. P., Laibinis, P. E. & Whitesides, G. M. Self-Assembled monolayers of alkanethiols on gold -comparisons of monolayers containing mixtures of short-chain and long-chain constituents with CH3 and CH2OH terminal groups. *Langmuir* **8,** 1330–1341 (1992).

[15] Smith, R. K. *et al.* Phase separation within a binary self-assembled monolayer on Au{111} driven by an amide-containing alkanethiol. *J. Phys. Chem. B* **105,** 1119–1122 (2001).

[16] Imabayashi, S., Gon, N., Sasaki, T.,Hobara,D. & Kakiuchi, T. Effect of nanometer-scale phase separation on wetting of binary self-assembled thiol monolayers on Au(111). *Langmuir* **14,** 2348–2351 (1998).

[17] Ingram, R. S.,Hostetler, M. J. & Murray, R. W. Poly-hetero-omega-functionalized alkanethiolate stabilized gold cluster compounds. *J.Am. Chem. Soc.* **119,** 9175–9178 (1997).

[18] Ulman, A. Formation and structure of self-assembled monolayers. *Chem. Rev.* **96,** 1533–1554 (1996).